Passive scalar mixing in modulated turbulence

Yuyao Yang, Robert Chahine, Robert Rubinstein, Wouter J.T. Bos

Passive scalar mixing in modulated turbulence

Yuyao Yang[a], Robert Chahine[a] Robert Rubinstein[b] and Wouter J.T. Bos[a]

[a]LMFA, CNRS, Ecole Centrale de Lyon, Université de Lyon, 69134 Ecully, France;
[b]Newport News, VA, USA

ARTICLE HISTORY
Compiled March 20, 2019

ABSTRACT
We investigate the mixing of a passive scalar in an isotropic turbulent flow in the presence of a time-periodic forcing. The results corroborate recent analytical predictions on the frequency dependence of the scalar variance and dissipation. In particular, when the modulation amplitude is large, it is shown that a low frequency modulation diminishes the mixing rate, whereas it enhances the transfer rate of kinetic energy, as compared to a flow with the same properties without an imposed temporal modulation of the forcing.

KEYWORDS
Turbulence, passive scalar, mixing rate, forcing protocol

1. Introduction

Is it possible to enhance the mixing rate of a turbulent flow by adding a periodic modulation to the mixing protocol? That is the main question we address in this investigation by considering the academic case of isotropic turbulence, mixing a passive scalar.

The mixing rate of a scalar quantity advected by a fluid is a key quantity in a wide range of applications. Increasing the mixing rate by changing the flow properties can have far reaching consequences in process-optimization. Whereas the mixing in laminar flows can often be studied analytically, and the mixing rate can be greatly enhanced by changing the boundary conditions [1] or the time-dependence of the flow [2], the turbulent case is in general far more complicated. It is not even known if it is possible to affect, in a controlled way, the mixing of a turbulent flow by changing the large-scale forcing.

If any understanding of the modification of turbulent mixing through time-dependent forcing is to be obtained, we think it is compulsory to look at the most simplified case. We consider therefore the academic case of periodically forced isotropic turbulence, advecting a passive scalar.

The influence of a time-periodic forcing on the turbulence itself is a relatively young problem, despite its obvious academic interest. Indeed, whereas first studies on oscillating turbulent pipe flows go back to the early seventies [3], first results on the response of a turbulent velocity field on a time-periodic isotropic forcing were only obtained in the beginning of the 2000s. The initial studies aimed at identifying a possible resonance

Email: wouter.bos@ec-lyon.fr

in the energy transfer process [4–6]. Direct numerical simulations [7,8] and experiments [9,10] were carried out to systematically investigate the response of the kinetic energy and dissipation rate to the forcing frequency. Analytical studies, using two-point closure techniques, allowed to explain the different scaling regimes of the time-dependent quantities [11] and assess the ability of engineering models to reproduce the different features [12].

Obviously it is extremely interesting to transpose these ideas to turbulent mixing. Inspired by DNS results on modulated turbulence [7], the application of particular forcing schemes to influence turbulent mixing was considered [13]. The forcing was introduced in different wavenumber bands in Fourier space to mimic the complex nature of turbulent flows generated by realistic objects. The influence of the so-generated flow on turbulent mixing was assessed by monitoring the wrinkling of level-sets of an advected scalar. Those results inspired several experimental investigations with application to turbulent combustion [14,15]. In the previous DNS study aiming at the assessment of the influence of the forcing type on mixing in turbulent flow [13], the spatial character of the forcing was modified, but no temporal modulation was applied. In the experiments the modulation was both spatial and temporal, and it is not straightforward to disentangle the different effects, so that it is not clear whether the observed effects were caused by the time-periodic nature of the experimental inlet conditions or the spatial complexity of the latter. The influence of the geometry of a large-scale forcing on mixing has thus already received some attention, but the temporal modulation of the flow was not considered in these studies.

In a recent paper [16], we carried out an analytical study of such a case: mixing in periodically forced turbulence. We showed that the second-order contributions of a perturbation analysis of the nonlinear transfer with respect to a modulation of the velocity forcing will lead to (1) an enhanced energy transfer (2) a reduced scalar transfer. Since the study was based on a simple turbulence closure and the perturbation analysis assumed small modulation amplitude, it is important to check the results in a more realistic setting, where the Navier-Stokes and advection-diffusion equations are not modeled, but directly evaluated. That is what will be done in the present investigation.

In the next section (section 2) we will outline the strategy to assess the influence of a periodic forcing on the mixing of a passive scalar, we will recall the analytical results and discuss the numerical tools. Then, in section 3 we will show and discuss the results, before concluding in section 4.

2. Definitions, predictions and numerical set-up

2.1. Description of the problem

We consider the Navier-Stokes equations for incompressible flow $\boldsymbol{u}$, mixing a passive scalar θ:

$$\frac{\partial}{\partial t}\boldsymbol{u} + \boldsymbol{u}\cdot\nabla\boldsymbol{u} = -\nabla P + \nu\nabla^2\boldsymbol{u} + \boldsymbol{f} \tag{1}$$

$$\nabla\cdot\boldsymbol{u} = 0 \tag{2}$$

$$\frac{\partial}{\partial t}\theta + \boldsymbol{u}\cdot\nabla\theta = D\nabla^2\theta + g, \tag{3}$$

where P is the pressure (normalized by a uniform density), ν and D are kinematic viscosity and diffusivity, respectively. The flow and the scalar field are kept in a statistically stationary state through an energy and scalar variance input $\boldsymbol{f}$, g acting at the large scales of the flow. The forcing $\boldsymbol{f}$ and g are acting at the same wavelength, so that there is one integral lengthscale L determining both the scalar and velocity dynamics. The forcing functions are chosen such that ensemble averaging (or phase-averaging), indicated by brackets $\langle . \rangle$, yields,

$$\langle f_i u_i \rangle \equiv p(t) = \overline{p} + \tilde{p}\cos(\omega t), \tag{4}$$

$$\langle g\theta \rangle \equiv p_\theta(t) = \overline{p}_\theta + \tilde{p}_\theta \cos(\omega t), \tag{5}$$

where the quantities p and p_θ denote the average kinetic energy and scalar variance injection rates. Overlined quantities denote time-averages and tilded quantities denote the amplitude of a periodic (non-zero frequency phase-averaged) contribution. The precise form of the forcing is given in the appendix.

In our study the flow domain is a spatially periodic box. In the present setting the evolution equations for the kinetic energy $k = \frac{1}{2}\left\langle |\boldsymbol{u}|^2 \right\rangle$ and the variance of the scalar $k_\theta = \frac{1}{2}\left\langle \theta^2 \right\rangle$ reduce to

$$\frac{dk}{dt} = p - \epsilon \tag{6}$$

$$\frac{dk_\theta}{dt} = p_\theta - \epsilon_\theta. \tag{7}$$

In these equations ϵ and ϵ_θ are the phase averaged dissipation of kinetic energy and scalar variance, respectively, defined by

$$\epsilon = \nu \left\langle \frac{\partial u_i}{\partial x_j} \frac{\partial u_i}{\partial x_j} \right\rangle \quad \text{and} \quad \epsilon_\theta = D \left\langle \frac{\partial \theta}{\partial x_j} \frac{\partial \theta}{\partial x_j} \right\rangle. \tag{8}$$

All the different statistical quantities of interest will in the following be decomposed into a time-averaged and a periodic component. Thereby the expressions of k and ϵ are

$$k(\omega, t) = \overline{k}(\omega) + \tilde{k}(\omega)\cos(\omega t + \phi_k), \tag{9}$$

$$\epsilon(\omega, t) = \overline{\epsilon}(\omega) + \tilde{\epsilon}(\omega)\cos(\omega t + \phi_\epsilon), \tag{10}$$

where ϕ indicates a phase-shift. Analogous expressions can be written for k_θ and ϵ_θ. It is of interest here to note that both the time-averaged quantities, such as $\overline{k}$ and the amplitudes of the periodic part like $\tilde{k}$ are in principle a function of the imposed forcing frequency ω. In the limit of small fluctuations, as considered in previous studies [11,12], it is only the tilded quantities which depend on the forcing frequency. This is the most important novelty of the present investigation, where we consider the influence of large modulation amplitudes on the frequency behaviour of the averaged quantities. Since all quantities $\overline{k}$, $\overline{\epsilon}$, $\overline{k_\theta}$, $\overline{\epsilon_\theta}$, $\tilde{k}$, $\tilde{\epsilon}$, $\tilde{k}_\theta$ and $\tilde{\epsilon}_\theta$ are a function of ω only, we will omit this dependence in the following.

The time-averaged balance equations for the kinetic energy and scalar variance are

given by

$$0 = \overline{p} - \overline{\epsilon} \tag{11}$$

$$0 = \overline{p}_\theta - \overline{\epsilon}_\theta, \tag{12}$$

and the periodic quantities evolve according to

$$-\omega\tilde{k}\sin(\omega t + \phi_k) = \tilde{p}\cos(\omega t) - \tilde{\epsilon}\cos(\omega t + \phi_\epsilon), \tag{13}$$

$$-\omega\tilde{k}_\theta\sin(\omega t + \phi_{k_\theta}) = \tilde{p}_\theta\cos(\omega t) - \tilde{\epsilon}_\theta\cos(\omega t + \phi_{\epsilon_\theta}). \tag{14}$$

In these expressions, we have assumed that all quantities will periodically oscillate around a mean value with a frequency ω. This was observed to be the case in our simulations. In previous works [5–8,11], the frequency dependence of $\tilde{k}$ and $\tilde{\epsilon}$ was investigated. The influence of the modulation on the time-averaged quantities $\overline{k}$ and $\overline{\epsilon}$ has not received any attention yet in the analytical and numerical studies, in particular since a linear perturbation analysis does not show any influence of the modulation on the averages. In the experimental studies [9,10] measurements were made of the average injection rate, but mostly aiming at the determination of a possible resonance. It is these average quanties that quantify the transfer rate.

Indeed one can introduce the transfer efficiency of kinetic energy χ as the inverse of the integral timescale

$$\chi = \frac{\overline{\epsilon}}{\overline{k}}. \tag{15}$$

The value of χ measures the efficiency of the energy transfer through the energy cascade. In our set-up, where the average dissipation should balance the average injection, it is therefore $1/\overline{k}$, which measures the efficiency.

In order to measure the transfer efficiency of the passive scalar, one can define the mixing rate χ_θ,

$$\chi_\theta = \frac{\overline{\epsilon}_\theta}{\overline{k}_\theta}, \tag{16}$$

measuring the efficiency of a flow to transfer scalar variance to diffusivity-dominated scales. Similarly, this quantity is in a steady state determined by $1/\overline{k}_\theta$.

2.2. Summary of analytical results

In this summary we will only consider the case where the kinetic energy injection is modulated $\tilde{p} \neq 0$, $\tilde{p}_\theta = 0$, and where the modulation frequency is small. For the high frequency analytical results we refer to references [11,16].

In reference [11] we derived using spectral closure theory the frequency dependence of the modulated part of the kinetic energy $\tilde{k}$ and viscous dissipation $\tilde{\epsilon}$. In the low frequency, or quasistatic limit, both quantities were predicted to tend to constant values, independent of the frequency,

$$\tilde{\epsilon} = \tilde{p} \tag{17}$$

$$\tilde{k} = \frac{2}{3}\alpha_p\bar{k}, \tag{18}$$

where the relative forcing amplitude is defined by

$$\alpha_p = \frac{\tilde{p}}{\bar{p}}. \tag{19}$$

More importantly, retaining second-order contributions in the perturbation analysis, we obtained estimates of the influence of the modulation on the time-averaged quantities, χ and χ_θ [16]. We will here give a simplified derivation of the results in [16]. For this analysis we will use the Taylor expression for the dissipation (or injection) rate

$$p \sim \frac{k^{3/2}}{L}, \tag{20}$$

with L the integral lengthscale. Combining this with our expression for the modulated forcing yields

$$k \sim (\overline{p} + \tilde{p}\cos(\omega t))^{2/3} L^{2/3}. \tag{21}$$

In our setting the forcing-scale is fixed, so that we find immediately,

$$\overline{k} \sim (\overline{p}L)^{2/3} \overline{(1 + \alpha_p \cos(\omega t))^{2/3}} \tag{22}$$

developing to second order gives

$$\overline{k} \sim (\overline{p}L)^{2/3} \left(1 - \frac{1}{18}\alpha_p^2\right), \tag{23}$$

which corresponds to the previous results [16], for $\alpha_p \ll 12$. Similarly, using the analog of the Taylor expression for the passive scalar,

$$p_\theta \sim \frac{k_\theta k^{1/2}}{L}. \tag{24}$$

and combining this with Taylor's relation (20) gives

$$k_\theta \sim \frac{p_\theta L^{2/3}}{p^{1/3}}. \tag{25}$$

to that one obtains

$$\overline{k}_\theta \sim \frac{\overline{p}_\theta L^{2/3}}{\overline{p}^{1/3}} \left(1 + \frac{1}{9}\alpha_p^2\right). \tag{26}$$

These expressions yield then the relations for the energy transfer and scalar mixing rate,

$$\frac{\chi}{\chi(\tilde{p}=0)} = \left(1 + \frac{1}{18}\alpha_p^2\right). \tag{27}$$

and

$$\frac{\chi_\theta}{\chi_\theta(\tilde{p}=0)} = \left(1 - \frac{1}{9}\alpha_p^2\right), \tag{28}$$

where $\chi(\tilde{p}=0)$ and $\chi_\theta(\tilde{p}=0)$ are the transfer efficiencies in the absence of modulation. These expressions show that a modulation of the forcing can influence the average value of the transfer efficiency. For the kinetic energy transfer χ, this effect is positive, whereas for the scalar mixing rate this effect is negative. These expressions also show that the relative strength of the forcing, $\alpha_p = \tilde{p}/\overline{p}$ must be large for the modulation to affect the transfer rates significantly. To illustrate: for $\alpha_p = 0.2$, it is found that $\chi/\chi(\tilde{p}=0) = 1.002$ and $\chi_\theta/\chi_\theta(\tilde{p}=0) = 0.996$, whereas these values change to 1.05 and 0.89 respectively for $\alpha_p = 1$.

The analytical predictions suggest thus that we can affect the mixing rate of a turbulent flow by modulating the energy input. However, the modulation increases the energy transfer rate but decreases the scalar transfer, which is the opposite of what is desirable in most applications. In general one would prefer a modification of the mixing protocol leading to better mixing, while consuming less kinetic energy. The analytical results suggest that a slow modulation will lead to more kinetic energy transfer, for a less efficient scalar transfer. The fact that a modulation enhances the transfer of energy, whereas the opposite is observed for the scalar variance is a direct consequence of the fact that k in expression (20) is proportional to $p^{2/3}$, whereas this exponent is negative in expression (25). Note further that in this derivation we have only considered the large-scale quantities p, p_θ, k, k_θ and L. Therefore these results are supposed to be robust even when the Schmidt number $Sc = \nu/D$ is non-unity, as long as the Péclet is sufficiently large for the large scales not to be affected by diffusion.

Indeed, the fact that relations (20) and (24) lead to the same results as a more detailed spectral analysis seems to indicate that, if we are in a regime where both the kinetic energy and passive scalar are dominated at the large scales by nonlinear transfer and not by visco-diffusive effects, the above arguments remain valid. Nevertheless, this remains fairly speculative and it would be interesting to test this by simulations at different Schmidt numbers. The parameter-space becomes thereby significantly larger and we will not consider these cases in the present work.

Since these predictions were obtained using a second-order perturbation of a simplified transfer model, it is important to check them numerically. Indeed, within the framework of a perturbation analysis, we consider that we measure the response of a system to an infinitesimal perturbation. In the case of a periodic perturbation the response is assumed to be at the same frequency as the perturbation, around the unaltered system. When the perturbation is large, the system itself can be affected importantly, and linear-response theory is no longer valid. In our case, a perturbation of the injection with an amplitude equal to the average injection cannot possibly be considered infinitesimal. It is therefore interesting to see if such a perturbation modifies the time-averaged properties of the flow, as suggested by expressions (27) and (28), obtained, as we said, from a second-order perturbation analysis.

2.3. Numerical set-up

A standard pseudospectral method is used to compute the velocity and scalar field in a space-periodic cubic domain of size 2π. A conventional 2/3 wavenumber truncation is used to eliminate the aliasing error and a third order Runge-Kutta, Total Variation

Diminishing scheme is used as time discretisation. The same code was used to study the mixing of temperature fluctuations in isotropic turbulence [17].

A total number of 46 simulations is carried out at two different values of the Taylor-scale Reynolds number, $R_\lambda = 32$ and 105 where $R_\lambda = \sqrt{20/3}(k/\sqrt{\nu\epsilon})$. The integral lengthscale will in the present investigation be taken proportional to the box-size, $L = 2\pi$. Since the forcing lenghtscale, which determines primarily the integral lengthscale, is fixed with respect to the boxsize, this choice is not supposed to qualitatively change the results.

A challenge in the study of the frequency response of turbulent flows is the convergence of the statistics. At low forcing frequencies the simulations become very long if a sufficient number of periods is to be resolved. At high frequencies the response to a periodic forcing will be shown to be small, so that also in this case long simulations are needed, not to resolve sufficient periods, but to be able to distinguish the frequency response from the turbulent fluctuations. Obtaining converged statistics is therefore challenging in both the small and large frequency limits.

Details on the numerical parameters and on the post-processing procedure are given in the Appendix.

3. Results

Two different cases will be considered: the case of mixing in a modulated turbulent velocity field ($\tilde{p} \neq 0$ and $\tilde{p}_\theta = 0$) and the case where only the scalar injection is modulated ($\tilde{p} = 0$ and $\tilde{p}_\theta \neq 0$).

3.1. Response of turbulence and mixing on a periodic kinetic energy input

In this section we consider the case where we only modulate the kinetic energy,

$$p = \overline{p} + \tilde{p}\cos(\omega t), \tag{29}$$

$$p_\theta = \overline{p_\theta}. \tag{30}$$

It will be shown that the modulation $\tilde{p}$ of the velocity field does also affect the mixing of the passive scalar.

3.1.1. Frequency response of the modulated kinetic energy and dissipation

The frequency response of $\tilde{k}$ and $\tilde{\epsilon}$ is shown in Fig. 1 for $R_\lambda = 32$. We compare in this figure the frequency responses for two different relative forcing amplitudes, $\alpha_p = \tilde{p}/\overline{p} = 0.2$ and $\alpha_p = 1$. In order to compare the frequency response for the different forcing amplitudes, we plot in these figures the quantities

$$k^* = \alpha_p^{-1}\frac{\tilde{k}}{\overline{k}} \quad \text{and} \quad \epsilon^* = \alpha_p^{-1}\frac{\tilde{\epsilon}}{\overline{\epsilon}} \tag{31}$$

as a function of frequency. Several observations can be made. Firstly, the 20% and 100% relative forcing amplitudes give results that superpose at almost all frequencies for both quantities. These observations seem to indicate that the results of the linear-perturbation analysis are robust enough to be transposable to the case where $\alpha_p = 1$,

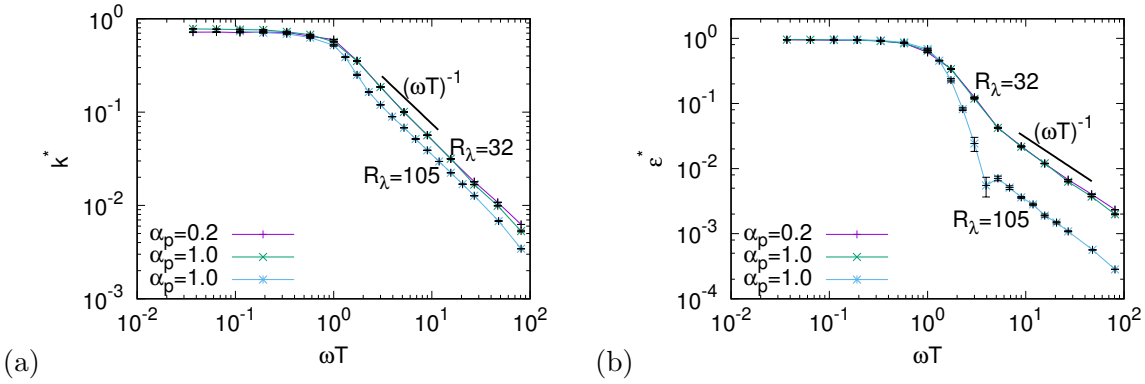

Figure 1. The frequency dependence of (a) $k^* = \frac{\tilde{k}}{\bar{k}}\alpha_p^{-1}$ and (b) $\epsilon^* = \frac{\tilde{\epsilon}}{\bar{\epsilon}}\alpha_p^{-1}$ as a function of ωT for $R_\lambda = 32$ and $R_\lambda = 105$, $\alpha_p = 0.2$ and $\alpha_p = 1$.

i.e., the case where the modulation amplitude has the same value as the mean value. Numerically, this is convenient, since the $\alpha_p = 1$ results allow to obtain results at a lower computational cost, and therefore, at higher Reynolds number, because the signal-to-noise ratio is larger.

Secondly, the powerlaw dependence proportional to ω^{-1} observed in previous investigations [7,11] is clearly reproduced both for $\tilde{k}$ and $\tilde{\epsilon}$. At small frequencies both $\tilde{k}$ and $\tilde{\epsilon}$ tend to constant values, as predicted [11], but unlike DNS results [7] at these frequencies, perhaps due to unconverged statistics in the simulations. Indeed, in one of the previous investigations [7], a local maximum was observed at low frequencies, suggestive of a resonance. This effect is not observed in our results, neither was it in the closure studies [11].

Furthermore, Figure 1 also illustrates the influence of the Reynolds number on the modulated kinetic energy and dissipation. It is observed that this influence is small for the modulated kinetic energy. However, for the dissipation this influence is larger, as was explained by the fact that the ω^{-1} asymptote is inversely proportional to the Reynolds number, since it corresponds to the direct influence of the viscous damping on the forced scales [11]. The intermediate zone between the low frequency plateau and the high frequency asymptote was theoretically predicted to be proportional to ω^{-3} for large Reynolds numbers [11]. This frequency range is too small here to be conclusive on the presence, or not, of such a power law.

3.1.2. Frequency response of the modulated scalar variance and its dissipation

The results on $\tilde{k}$ and $\tilde{\epsilon}$ in the foregoing section are in agreement with previous work (except for the small local maximum observed in DNS [7]). In Figure 2 we evaluate quantities which have not received any attention yet in experiments and simulations: $\tilde{k}_\theta$ and $\tilde{\epsilon}_\theta$. It is observed that the large-frequency asymptotes predicted in our previous investigation [16] are well reproduced. More specifically it is observed that the scalar variance contains a periodic component which is constant at low frequencies, and rapidly drops off at high frequencies, following a powerlaw proportional to ω^{-3}. The periodic part of the scalar dissipation behaves as $|\tilde{\epsilon}_\theta| = \omega|\tilde{k}_\theta|$ as is illustrated in figure 2, where for ω tending to zero $\tilde{\epsilon}_\theta$ is proportional to ω, and for large values of ω the asymptotic slope is proportional to ω^{-2}. It seems that the analytical predictions based on the linear perturbation of a simple flux closure for the nonlinear transfer is sufficient

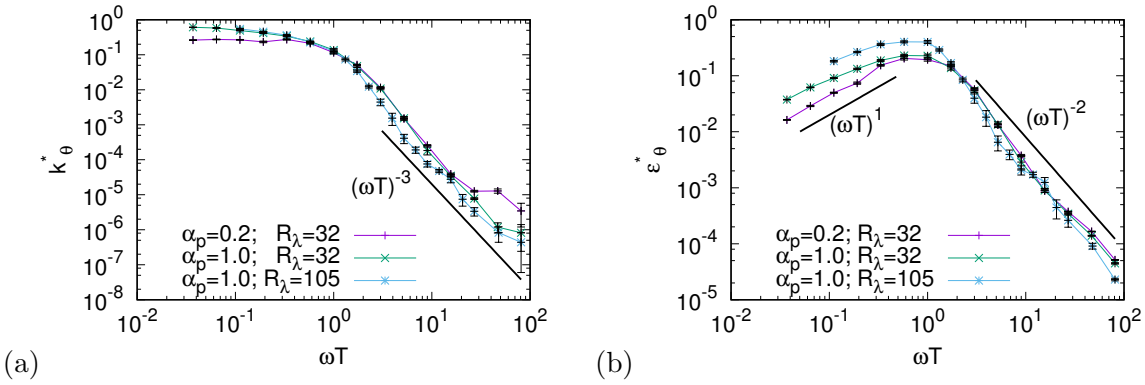

Figure 2. Frequency response of (a) the modulated scalar variance $k^*_\theta = \frac{\tilde{k}_\theta}{\overline{k}_\theta}\alpha_p^{-1}$ and (b) modulated scalar dissipation $\epsilon^*_\theta = \frac{\tilde{\epsilon}_\theta}{\overline{\epsilon}_\theta}\alpha_p^{-1}$ for $R_\lambda = 32$ and $R_\lambda = 105$. The relative forcing amplitude is $\alpha_p = 1$.

to predict the small and large frequency asymptotes of both $\tilde{k}_\theta$ and $\tilde{\epsilon}_\theta$.

3.1.3. Influence of the modulation on the mixing and transfer rates

We now present the most important results of this investigation. In Figure 3, the influence of the modulation is shown on the quantities χ and χ_θ. Our forcing scheme is designed to keep the average rate of ϵ and ϵ_θ constant. Thereby, in none of our simulations, the values of $\overline{\epsilon}(\omega)$ and $\overline{\epsilon}(\tilde{p} = 0)$ differ more than 2%. The transfer and mixing rates are then determined by the variations in $\bar{k}(\omega)$ and $\bar{k}_\theta(\omega)$ (see equations (15) and (16)). It is shown that for $\alpha_p = 0.2$, no clear modification of the mixing and transfer rate is observed. Indeed, the analytical study predicted the effect for this value of α_p to be less than 0.5%, well below the statistical errors induced by the time-averaging. However, for $\alpha_p = 1$, a clear effect is observed, of the order of $+7\%$ for χ and -20% for χ_θ. These are of the same order of magnitude, but slightly larger than the analytically predicted values $(+5\%, -11\%)$. Clearly the analytical study predicted the correct tendencies and order of magnitude of the influence of the modulation of the mixing and transfer rate. The fact that the numerical values are not exactly predicted cannot be considered very surprising given the nature of the simplifications in the analytical study.

These results confirm thus that the modulation of the velocity field can affect the average transfer and mixing rates in the low frequency limit. The origin of this effect is the nonlinear dependence of the kinetic energy and scalar variance on the forcing, $k \sim p^{2/3}$, $k_\theta \sim p^{-1/3}$, as follows from relations (21) and (25). The Reynolds number does not seem to be an important parameter for the values we considered, which illustrates the robustness of the observations.

3.2. Modulation of the scalar injection

For completeness, we now consider the case where we only modulate the scalar input,

$$p = \overline{p}, \tag{32}$$

$$p_\theta = \overline{p_\theta} + \tilde{p}_\theta \cos(\omega t). \tag{33}$$

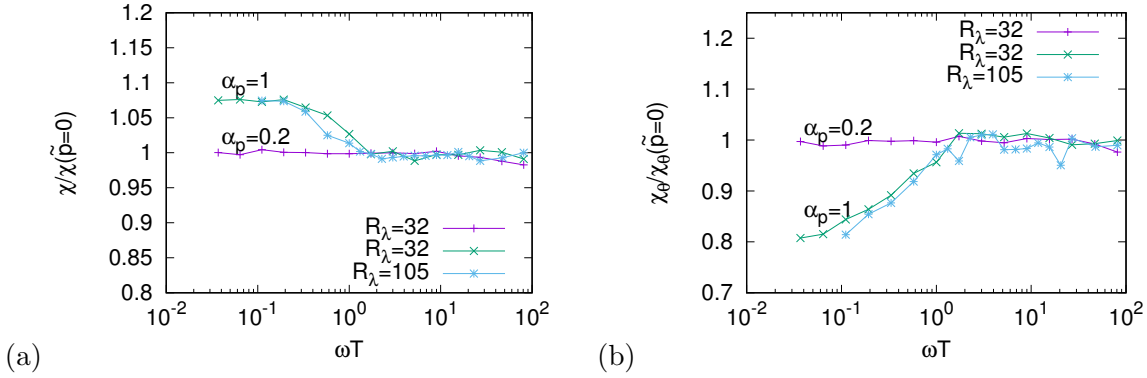

Figure 3. Influence of the large-scale modulation on the transfer-rate χ and mixing-rate χ_θ, for $R_\lambda = 32$ and $R_\lambda = 105$, $\alpha_p = 0.2$ and $\alpha_p = 1$.

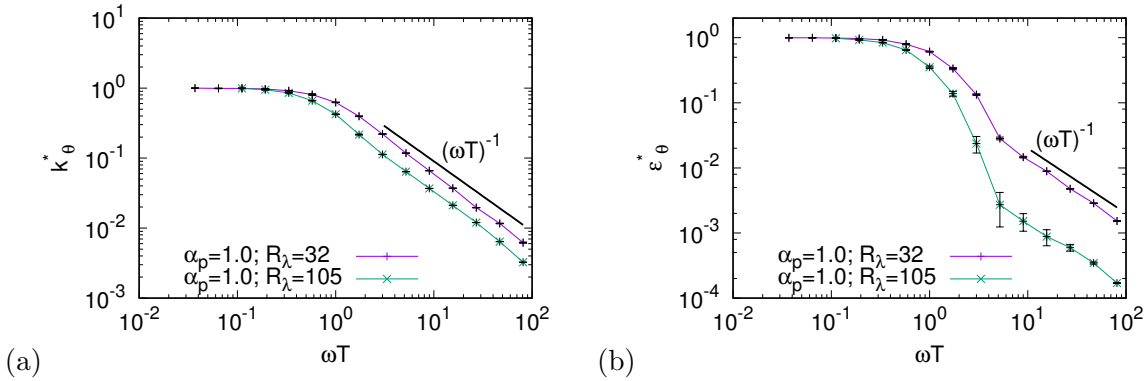

Figure 4. Amplitudes of the modulated scalar variance $k^*_\theta = \frac{\tilde{k}_\theta}{\bar{k}_\theta}\alpha_p^{-1}$ and (b) modulated scalar dissipation $\epsilon^*_\theta = \frac{\tilde{\epsilon}_\theta}{\bar{\epsilon}_\theta}\alpha_p^{-1}$ as a function of ωT for the case of a modulated scalar injection. Results for $R_\lambda = 32$ and $R_\lambda = 105$, both at $\alpha_p = 1$.

Naturally the modulation $\tilde{p}_\theta$ should not influence the velocity field and we therefore only evaluate the influence of the modulation on the scalar quantities.

In Figure 4 we show the results for $k^*_\theta = \alpha_p^{-1}\tilde{k}_\theta/\bar{k}_\theta$ and dissipation $\epsilon^*_\theta = \alpha_p^{-1}\tilde{\epsilon}_\theta/\bar{\epsilon}_\theta$ as a function of the modulation frequency for $\alpha_p = 1$, $R_\lambda = 32$ and $R_\lambda = 105$. A very close similarity with the results for k^* and ϵ^* in Figure 1 is observed. In particular the small and large frequency asymptotes are identical. Indeed, the reasonings leading to the prediction of the frequency behaviour of the kinetic energy and dissipation [11] can be extended to the case of the passive scalar, in particular in the limit of the linear response approximation.

4. Conclusion

In this manuscript, we have answered to the question whether a periodic modulation of a turbulent flow changes its mixing properties. It was clearly shown that for large modulation amplitudes, the modulation affects the energy transfer positively, whereas it diminishes the mixing rate, as was predicted in a recent analytical study [16]. The

average mixing rate was shown to decrease by approximately 20%, for two distinct Reynolds numbers, whereas the energy transfer rate increases by approximately 7%. This result shows that in most applications where an efficient mixing is required for a minimum amount of energy, the modulation of the velocity field is not a good idea. We should however mention that these results concern the case of isotropic turbulence and that a possible mixing enhancement by the modulation of spatially inhomogeneous mixing devices cannot be excluded. However, we show here that it is not the heart of the turbulent mechanism, the energy and scalar cascade, which is affected in the desired way by the modulation of an isotropic forcing.

It can now be asked how our findings can be assessed in experiments. Experimental investigations of mixing in isotropic turbulence have focused mainly on grid-turbulence. In such flows the turbulence is decaying from initial conditions, generated at the grid. Active-grids have been used to modulate turbulence [10], and to generate high Reynolds number flow in which to study scalar mixing [18]. However, the combination of these two, i.e., using modulated active grids to generate a turbulent flow in which small temperature fluctuations are injected, would constitute a perfect set-up to check the results of the present investigation in a real life flow.

Given the negative results obtained here one might question if it is worth to set up such experiments. Indeed, it might, and we want to finish this investigation by a positive note for those who want to enhance mixing by temporal modulation. Indeed, there might be a way to enhance the mixing by modulation in the current framework. To understand this reconsider equations (20) and (25),

$$k(t) \sim (p(t)L)^{2/3},$$
$$k_\theta(t) \sim \frac{p_\theta(t)L^{2/3}}{p(t)^{1/3}}.$$

The average kinetic energy transfer rate is in the current investigation influenced through the temporal modulation, because k is nonlinear dependent on p. On the contrary, k_θ will not be affected by a modulated forcing of the scalar input p_θ, since their inter-dependence is linear. However, k_θ depends nonlinearly on L. Therefore, there might be a chance that the temporal modulation of the integral scale L could enhance the mixing. Indeed, introducing a modulated integral scale,

$$L = \overline{L}(1 + \alpha_L \cos(\omega t)) \tag{34}$$

the analysis in section 2.2 leads straightforwardly to

$$\overline{k} \sim \overline{p}^{2/3}\overline{L}^{2/3}\left(1 - \frac{1}{18}\alpha_p^2\right)$$
$$\overline{k}_\theta \sim \frac{\overline{p}_\theta \overline{L}^{2/3}}{\overline{p}^{1/3}}\left(1 - \frac{1}{18}\alpha_p^2\right). \tag{35}$$

And therefore, in this case, both the transfer of kinetic energy and of scalar variance are enhanced. We note that we have assumed here that it is possible to modulate L, while keeping p and p_θ constant. Investigating whether this is realizable and if such a modulation leads to improved mixing seems to be a promising direction for further research.

Appendix: further details on the numerical simulations and postprocessing procedure

The numerical simulations are carried out at two different resolutions, corresponding to different values of the Reynolds number. First, low resolution simulations at a spatial resolution of 64^3 are performed with kinematic viscosity $\nu = 0.009$, corresponding to a Taylor Reynolds number $R_\lambda = 32$, with eddy turn-over time $T = 1.949$. The resolution allows to resolve the smallest scales upto $k_{max}\eta = 0.93$. Another set of simulations is carried out at a resolution of $N^3 = 256^3$ gridpoints, kinematic viscosity $\nu = 0.0009$; Taylor Reynolds number $R_\lambda = 105$; eddy turn-over time $T = 2.317$ and $k_{max}\eta = 0.97$, where $\eta = \nu^{3/4}/\epsilon^{1/4}$ and k_{max} the largest resolved wavenumber. In all simulations the Schmidt number $Sc \equiv \nu/D = 1$.

The Fourier-transformed velocity and scalar field are denoted by $\hat{u}_i$ and $\hat{\theta}$, respectively. The forced Fourier-modes are the modes in the range $0.5 < |\boldsymbol{\kappa}| \leq 2.5$. Only for these modes the forcing terms are non-zero and have the form

$$\hat{f}_i(\boldsymbol{\kappa}, t) = \frac{1}{N_F} \frac{\hat{u}_i(\boldsymbol{\kappa}, t)}{|\hat{\boldsymbol{u}}(\boldsymbol{\kappa}, t)|^2} (\overline{p} + \tilde{p}\cos(\omega t)) \tag{36}$$

$$\hat{g}(\boldsymbol{\kappa}, t) = \frac{1}{N_F} \frac{\hat{\theta}(\boldsymbol{\kappa}, t)}{\left|\hat{\theta}(\boldsymbol{\kappa}, t)\right|^2} (\overline{p}_\theta + \tilde{p}_\theta \cos(\omega t)), \tag{37}$$

with N_F the total number of forced modes. These forcing schemes will result in a statistically isotropic velocity and scalar field.

Previous investigations [7,11] focused in particular on the linear response of turbulence on a periodic modulation. In this limit linearized equations around a given equilibrium allow to analytically derive certain results. The verification of such results is not straightforward in the nonlinear regime, where the perturbation is large. Ideally, to investigate the linear response of a turbulent flow, the amplitude of the forcing should be chosen small compared to the amplitude of the steady part of the forcing ($\alpha_p \equiv \tilde{p}/\bar{p} \ll 1$). However, since the turbulent fluctuations are in this case much larger than the periodic response, very long simulations should be carried out to obtain an estimate of the frequency response. In particular at large frequencies, where the frequency response will be shown to drop rapidly as a function of frequency this would impose prohibitively long computations. A compromise is to consider a larger modulation amplitude. In this study, as in a previous DNS investigation [7], we use $\alpha_p \equiv \tilde{p}/\bar{p} = 0.2$. This allows to obtain converged statistics for a large range of frequencies at a reasonable computational cost for low Reynolds number ($R_\lambda = 32$). For higher Reynolds number this already leads to prohibitively long simulations. Therefore we have carried out another set of simulations with a relative modulation amplitude $\alpha_p = 1$. Even though this certainly violates the linear perturbation assumption, we will show that the frequency-response of the modulated quantities is not quantitatively altered. We will further show that this has an interesting direct influence on the time-averaged quantities.

Before extracting the frequency response of the simulations, the flow was simulated for approximately 10 eddy turn-over times to obtain a statistically steady state. It proved convenient to determine the amplitude of the periodic response by using a Fourier-transform of the signal. Before Fourier-transforming the time-series of a given quantity, a hanning window function is applied to the signal to eliminate the aliasing

error at high frequencies due to the finite length of the signal. In the frequency spectra, if the simulations are carried out for a sufficiently long time-interval, the amplitude of the periodic response is easily identified by a sharp peak. Comparing the value of this peak to the neighbouring values in the spectrum gives a direct estimate of the signal-to-(turbulent)-noise ratio. In all simulations the value of the peak at the considered frequency was at least ten times the value of the neighbouring values in the spectra. In particular, it was observed that the main response of the considered quantities appeared at the forcing frequency and that subharmonic contributions were negligible.

For the phase averaged amplitudes, error-bars are added to the datapoints in the figures, computed from the signal to noise ratio. In most cases, this error-bar is smaller than the size of the symbols used in the figures. The time-averaged value is conveniently estimated from the $\omega = 0$ component of the spectrum.

The different simulations we have carried out are documented in table 1.

acknowledgments

We gratefully acknowledge support from the PMCS2I (Pôle de Modlisation et Calcul en Science de l'Ingnieur et de l'Information), computing center of the Ecole Centrale de Lyon.

References

[1] Gouillart E, Kuncio N, Dauchot O, et al. Walls inhibit chaotic mixing. Phys Rev Lett. 2007;99(11):114501.
[2] Aref H. Stirring by chaotic advection. J Fluid Mech. 1984;143:1.
[3] Gerrard J. An experimental investigation of pulsating turbulent water flow in a tube. Journal of Fluid Mechanics. 1971;46(1):43–64.
[4] Lohse D. Periodically kicked turbulence. Phys Rev E. 2000;62:4946.
[5] von der Heydt A, Grossmann S, Lohse D. Response maxima in modulated turbulence. Phys Rev E. 2003;67:046308.
[6] von der Heydt A, Grossmann S, Lohse D. Response maxima in modulated turbulence. ii. numerical simulations. Phys Rev E. 2003;68:066302.
[7] Kuczaj AK, Geurts BJ, Lohse D. Response maxima in time-modulated turbulence: Direct numerical simulations. Europhys Lett. 2006;73:851.
[8] Kuczaj A, Geurts B, Lohse D, et al. Turbulence modification by periodically modulated scale-dependent forcing. Computers & Fluids. 2008;37(7):816–824.
[9] Cadot O, Titon J, Bonn D. Observation of resonances in modulated turbulence. J Fluid Mech. 2003;485:161.
[10] Cekli H, Tipton C, van de Water W. Resonant enhancement of turbulent energy dissipation. Phys Rev Lett. 2010;105(4):044503.
[11] Bos WJT, Clark T, Rubinstein R. Small scale response and modeling of periodically forced turbulence. Phys Fluids. 2007;19:055107.
[12] Rubinstein R, Bos WJT. On the unsteady behavior of turbulence models. Phys Fluids. 2009;21:041701.
[13] Kuczaj AK, Geurts BJ. Mixing in manipulated turbulence. J Turbul. 2006;7:N67. Available from: http://dx.doi.org/10.1080/14685240600827534.
[14] Verbeek A, Stoffels G, Bastiaans R, et al. Optimization of combustion in gas turbines by applying resonant turbulence. In: International Gas Union Research Conference, IGRC 2011. Foundation IGRC; 2011. Available from: http://doc.utwente.nl/79377/.

[15] Verbeek AA, Bouten TW, Stoffels GG, et al. Fractal turbulence enhancing low-swirl combustion. Combustion and Flame. 2015;162(1):129–143.
[16] Bos W, Rubinstein R. Mixing in modulated turbulence. Analytical results. Comput Fluids. 2017;.
[17] Bos WJT, Chahine R, Pushkarev A. On the scaling of temperature fluctuations induced by frictional heating. Phys Fluids. 2015;24:015108.
[18] Mydlarski L, Warhaft Z. Passive scalar statistics in high Peclet number grid turbulence. J Fluid Mech. 1998;358:135.

ωT	N	t	α_p	R_λ
0	0	800	0.2	32
0.037	4	1316	0.2	32
0.064	8	1519	0.2	32
0.11	8	877	0.2	32
0.19	8	506	0.2	32
0.33	8	292	0.2	32
0.57	8	169	0.2	32
1	15	183	0.2	32
1.7	90	633	0.2	32
3	180	731	0.2	32
5	540	1266	0.2	32
9	360	487	0.2	32
16	810	633	0.2	32
27	1080	487	0.2	32
47	110	29	0.2	32
81	200	30	0.2	32
0	0	800	1	32
0.037	4	1316	1	32
0.064	8	1519	1	32
0.11	8	877	1	32
0.19	8	506	1	32
0.33	8	292	1	32
0.57	8	169	1	32
1	15	183	1	32
1.7	35	246	1	32
3	60	243	1	32
5	105	246	1	32
9	180	243	1	32
16	315	246	1	32
27	540	243	1	32
47	945	246	1	32
81	1800	271	1	32
0	0	40	1	105
0.11	2	262	1	105
0.19	3	227	1	105
0.33	3	131	1	105
0.57	3	76	1	105
1	2	29	1	105
1.7	6	50	1	105
3	12	58	1	105
5	54	151	1	105
9	108	175	1	105
16	54	50	1	105
27	108	58	1	105
47	162	50	1	105
81	324	58	1	105

Table 1. Simulation parameters: normalized frequency ωT, number of simulated periods N, simulated time-interval t, relative forcing amplitude α_p and Reynolds number R_λ.